

Performance and robustness assessment of H_∞ active anti-roll bar control system by using a software environment

Van Tan Vu* Peter Gaspar**

* Department of Automotive Mechanical Engineering, University of Transport and Communications, Hanoi, Vietnam. E-mail: vvtan@utc.edu.vn

** Systems and Control Laboratory, Institute for Computer Science and Control, Hungarian Academy of Sciences, Kende u. 13-17, H-1111 Budapest, Hungary. E-mail: gaspar@sztki.mta.hu

Abstract: The active anti-roll bar system has been proven to be one of the most effective solutions to improve roll stability of heavy vehicles. In a previous work, the authors proposed an H_∞ controller for this system. The Genetic Algorithms method was used to handle the vehicle roll stability and the energy consumption of the actuators via the Pareto optimality. This paper aims to assess the overall effectiveness of the proposed controller with nonlinear heavy vehicle models, which are already set up in the TruckSim[®] software. The controller is then evaluated in hard conditions to show the high performance and robust with the nonlinearity effects, such as the load distribution between the two axles, the side wind gusts and the abrupt steering. To conduct testing of the H_∞ active anti-roll bar control system, we propose a co-simulation structure between TruckSim[®] and Simulink[®]: the nonlinear vehicle model is determined from TruckSim[®], based on using the block S-function of Simulink. Meanwhile, the controller and the actuators are built directly in the *Matlab*/Simulink[®] environment. The validation results are made through two different types of heavy vehicles: a tour bus and a truck, using a selection of different velocities and scenarios. The results show that by using the H_∞ active anti-roll bar control system, in comparison to the passive anti roll bar system, roll stability is improved to minimise the risk of vehicle rollover.

Keywords: Vehicle dynamics, Active anti-roll bar control, Rollover, H_∞ control, TruckSim[®].

1. INTRODUCTION

Heavy vehicles are the main transportation system of goods via roads worldwide. Many studies have reported that a significant proportion of serious road accidents involve lack of vehicle roll stability. Therefore, safety issues with these vehicles have become increasingly important. Rollover accidents mostly involve heavy vehicles (single unit, articulated vehicles) and occur on highways. Three major causes of rollover have been identified: sudden course deviation, excessive speed on curves and shifting load. It is usually difficult for the driver to sense the rollover behaviour, especially a tractor semi-trailer combination. Rollover accidents can be classified into four categories: preventable, potentially preventable, non-preventable and preventable unknown. It is worth noting that half of the rollover accidents are not preventable by driver action alone. This highlights the need for an active safety system for heavy vehicles (Hussain et al. (2005), Bouteldja (2004)).

There are several active intervention systems in vehicle dynamics that have been proposed, such as active anti-roll bar, active steering, active braking, active suspension, or a combination of them. Of these systems, the active anti-roll bar system is the most common method used to improve roll stability of heavy vehicles. Several control methods applied for this system include: Optimal control (Sampson and Cebon (2003a), Miege and Cebon (2005b), Yu et al. (2008)); Neural network control (Boada et al. (2007)); Robust control (*LPV*) (Gaspar et al. (2005)).

One of the most difficult aspects when researching the active

anti-roll bar system is to evaluate its effectiveness on the high nonlinear level of the vehicle model, especially on real vehicles. This system was validated for a real long combination heavy vehicles at the University of Cambridge in UK. They succeeded in studying theoretical simulations and the Cambridge Vehicle Dynamics Consortium sponsored the construction of the experimental vehicle. The experimental results clearly demonstrated the effectiveness of this system for improving roll stability of a articulated vehicle (Miege and Cebon (2005b), Miege and Cebon (2005a)).

Several studies of heavy vehicle stability have considered the TruckSim[®] software as an effective solution for evaluating the active control systems. In (Yu et al. (2008)), the authors used TruckSim to evaluate the rollover threat warning system based on the time-to-rollover metric. Also in (Qu et al. (2018), Islam et al. (2015), Ashfaq et al. (2017)), the closed-loop vehicle dynamic simulation model was established using TruckSim. These algorithms show that these heavy vehicles are less susceptible to rollover behavior. They also provide valuable guidelines on the selection of dynamic vehicle models using control algorithm development, design optimization and linear stability analysis for multi-trailer articulated heavy vehicles with active safety systems.

In the previous work (Vu et al. (2017b)), we designed an H_∞ active anti-roll bar control system using the integrated model for a single unit heavy vehicle. The aim is to improve the vehicle roll stability. The Genetic algorithms (GAs) method is then applied to find the optimal weighting functions solving the

multi-criteria optimization H_∞ control problem. Thanks to GAs, the conflicting objectives between the normalized load transfers and the input currents are handled using only one single high level parameter.

This paper validates the H_∞ active anti-roll bar control system proposed in (Vu et al. (2017b)) with the nonlinear vehicle model by using TruckSim[®] software. The main contributions is listed as follows:

- We propose a co-simulation between *Matlab/Simulink*[®] and TruckSim[®]. It allows the synthesis of the H_∞ active anti-roll bar controller in *Matlab/Simulink*[®] environment, and the nonlinear high order vehicle model is taken from TruckSim[®] by using the block S-function of Simulink.
- The validation is done for the four cases of the single unit heavy vehicle (4×2) (a tour bus and a truck in unloaded and fully loaded states) with different velocities and scenarios. The simulation results show that the H_∞ active anti-roll bar control system drastically improved vehicle roll stability to prevent the rollover phenomenon. This result confirms that the H_∞ active anti-roll bar control system proposed in (Vu et al. (2017b)) is really effective.

The paper is organised as follows: Section 2 summarizes the vehicle modelling and the H_∞ robust control synthesis to prevent rollover of heavy vehicles. Section 3 presents the co-simulation structure between TruckSim[®] and Simulink[®]. Section 4 shows the validation results of the H_∞ active anti-roll bar control system with a tour bus and a truck. Finally, some conclusions an perspectives are drawn in section 5.

2. H_∞ ACTIVE ANTI-ROLL BAR CONTROLLER DESIGN

In this section, we briefly summarize the integrated model (four Electronic Servo-Valve Hydraulic (ESVH) actuators in a linear single unit heavy vehicle yaw-roll model) (Vu et al. (2017a)) and the H_∞ controller design for the active anti-roll bar system (Vu et al. (2017b)). To accurately assess the effectiveness of the active anti-roll bar system in preventing the vehicle rollover phenomenon, we use the value of the interacting forces between the wheel and the road in the vertical direction (the tyre force in the z direction).

$$\left\{ \begin{array}{l} mv(\dot{\beta} + \dot{\psi}) - m_s h \ddot{\phi} = F_{yf} + F_{yr} \\ -I_{xz} \ddot{\phi} + I_{zz} \ddot{\psi} = F_{yf} l_f - F_{yr} l_r \\ (I_{xx} + m_s h^2) \ddot{\phi} - I_{xz} \ddot{\psi} = m_s g h \phi + m_s v h (\dot{\beta} + \dot{\psi}) \\ -k_f(\phi - \phi_{tf}) - b_f(\dot{\phi} - \dot{\phi}_{tf}) + 2l_{act} A_p \Delta P_f \\ -k_r(\phi - \phi_{tr}) - b_r(\dot{\phi} - \dot{\phi}_{tr}) + 2l_{act} A_p \Delta P_r \\ -rF_{yf} = m_{uf} v(r - h_{uf})(\dot{\beta} + \dot{\psi}) + m_{uf} g h_{uf} \phi_{tf} - k_{tf} \phi_{tf} \\ + k_f(\phi - \phi_{tf}) + b_f(\dot{\phi} - \dot{\phi}_{tf}) + 2l_{act} A_p \Delta P_f \\ -rF_{yr} = m_{ur} v(r - h_{ur})(\dot{\beta} + \dot{\psi}) - m_{ur} g h_{ur} \phi_{tr} - k_{tr} \phi_{tr} \\ + k_r(\phi - \phi_{tr}) + b_r(\dot{\phi} - \dot{\phi}_{tr}) + 2l_{act} A_p \Delta P_r \\ \frac{V_t}{4\beta_e} \dot{\Delta P}_f + (K_P + C_{1p}) \Delta P_f - K_x X_{vf} \\ + A_p l_{act} \dot{\phi} - A_p l_{act} \dot{\phi}_{uf} = 0 \\ \dot{X}_{vf} + \frac{1}{\tau} X_{vf} - \frac{K_v}{\tau} u_f = 0 \\ \frac{V_t}{4\beta_e} \dot{\Delta P}_r + (K_P + C_{1p}) \Delta P_r - K_x X_{vr} \\ + A_p l_{act} \dot{\phi} - A_p l_{act} \dot{\phi}_{ur} = 0 \\ \dot{X}_{vr} + \frac{1}{\tau} X_{vr} - \frac{K_v}{\tau} u_r = 0 \end{array} \right. \quad (1)$$

2.1 Vehicle modelling

The dynamic equations of the integrated model include the differential equations of the yaw-roll model (the lateral dynamics, the yaw moment, the roll moment of the sprung mass, the roll moment of the front and the rear unsprung masses) and the differential equations of the ESVH actuators. They are defined as equation (1).

The motion differential equations (1) can be rewritten in the LTI state-space representation as follows:

$$\dot{x} = A.x + B_1.w + B_2.u \quad (2)$$

where the state vector is chosen as:

$$x = [\beta \ \psi \ \phi \ \dot{\phi} \ \phi_{uf} \ \phi_{ur} \ \Delta P_f \ X_{vf} \ \Delta P_r \ X_{vr}]^T$$

$w = [\delta_f]^T$ the exogenous disturbance, $u = [u_f \ u_r]^T$ the control inputs, and A, B_1, B_2 the model matrices.

2.2 H_∞ controller design

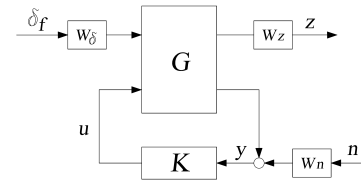


Fig. 1. H_∞ active anti-roll bar system: closed-loop structure.

Figure 1 shows the closed-loop structure of an H_∞ control designed for the active anti-roll bar system. In the diagram, G is the nominal model, K the controller, z the performance output, u the control input, y the measured output, n the measurement noise, δ_f the disturbance signal (steering angle) and W_δ, W_z, W_n the weighting functions.

The aim is to design a controller K that reduces the signal transmission path from disturbances δ_f to performance outputs z and also stabilizes the closed-loop system. The H_∞ problem is to find K which minimizes γ such that

$$\|\mathcal{F}_l(P, K)\|_\infty < \gamma \quad (3)$$

where P is generalized system. By minimizing a suitably weighted version of (3), the control aim is achieved.

From the closed-loop structure shown in Figure 1, the LTI state-space representation in equation (2) can be written in this form:

$$\begin{bmatrix} \dot{x} \\ z \\ y \end{bmatrix} = \begin{bmatrix} A & B_1 & B_2 \\ C_1 & D_{11} & D_{12} \\ C_2 & D_{21} & D_{22} \end{bmatrix} \begin{bmatrix} x \\ w \\ u \end{bmatrix} \quad (4)$$

where $w = [\delta_f \ n]$ is the exogenous input vector, $u = [u_f \ u_r]^T$ the control input vector, $z = [u_f \ u_r \ R_f \ R_r \ a_y]^T$ the performance output vector, $y = [a_y \ \dot{\phi}]^T$ the measured output vector. here $R_{f,r}$ are the normalized load transfers at the two axles, defined as: $R_f = \frac{k_{uf} \phi_{uf}}{l_w F_{zf}}$, $R_r = \frac{k_{ur} \phi_{ur}}{l_w F_{zr}}$ with $F_{zf,r}$ the total axle load, $k_{uf,r}$ the stiffness of the tyres, $\phi_{uf,r}$ the roll angles of the unsprung masses at both axles, l_w the half of the vehicle's width. The weighting functions of the closed-loop structure are:

$W_z = \text{diag}[W_{zuf}, W_{zur}, W_{zRf}, W_{zRr}, W_{za}]$, the weighting functions matrix represents the performance output, and its elements are defined in Table 1.

$W_n = \text{diag}[0.01(m/s^2), 0.01(^0/sec)]$, the noise weight represents for the lateral acceleration and the roll rate (Gaspar et al., 2004). The input scaling weight $W_\delta = \pi/180$ corresponds to a 1^0 steering angle command.

Table 1. The weighting functions for the performance output (Vu et al. (2017b)).

	W_{zUf}	W_{zUr}	W_{zRf}	W_{zRr}	W_{za}
Value	0.066	0.072	0.616	0.482	$0.492s + 202.316$ $455.747s + 0.544$

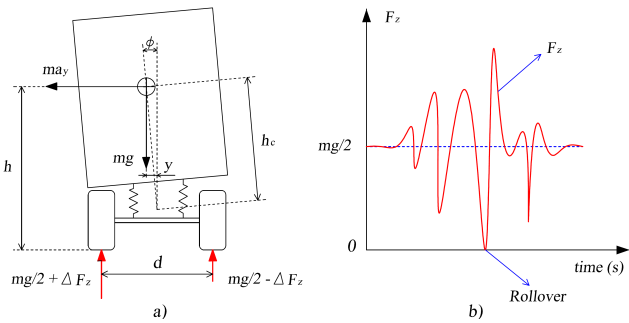


Fig. 2. Tyre force in the Z direction.

2.3 Performance criteria

In this study, to evaluate the rollover behavior of a vehicle, we use the tyre force in the Z direction at each wheel, defined as follows:

$$F_z = \frac{mg}{2} \pm \Delta F_z \quad (5)$$

where ΔF_z is the load transfer and $\frac{mg}{2}$ the static load at each wheel. The value of the tyre force in the Z direction fluctuates around the static load. In Figure 2, we can see that when the value $F_z = 0$, the wheel will start to lift off from the road and at that time we can consider that vehicle rollover has occurred.

3. CO-SIMULATION: TRUCKSIM[®] AND SIMULINK[®]

TruckSim[®] software is one of the three main products from the Mechanical Simulation Corporation. It predicts the performance of vehicles in response to driver control inputs (steering, accelerators, brakes, clutch, and gear shifting) in a given environment (road geometry, coefficients of friction, wind). In terms of performance factors, we can consider the following: vehicle motions, forces, and moments involved in acceleration, handling and braking. There are many main applications of TruckSim[®] such as: Electronic Stability Control, ABS Braking, Active Suspension, Autonomous Driving, Anti-roll Controls, Vehicle to Vehicle Communications, etc. Here, we are interested in the anti-roll bar control system. To survey the control systems by using the nonlinear vehicle model from TruckSim[®], usually a co-simulation is used.

3.1 Co-simulation structure

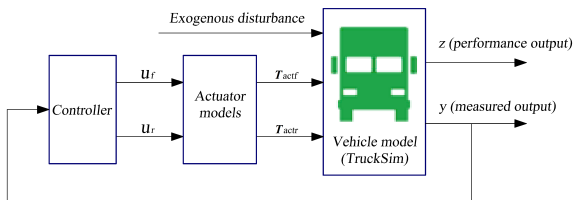


Fig. 3. Diagram of TruckSim[®]-Simulink[®] Co-Simulation.

In this paper, the authors use the co-simulation between Matlab/Simulink[®] and TruckSim[®], the diagram is shown in Figure 3. The nonlinear vehicle model is determined from TruckSim[®], based on using the block S-function of Simulink[®]. Meanwhile, the controller and the actuators are

built directly in Matlab/Simulink[®] environment. The output of the block S-function represented for the nonlinear vehicle model includes the performance and measurement outputs. We consider the two measurement outputs which are the lateral acceleration and the roll rate of the sprung mass. The input of the block S-function includes the exogenous disturbance and the two auxiliary moments from the active anti-roll bar system at both axes.

In the co-simulation between Simulink[®] and TruckSim[®], there are two following solutions for the steering angle:

- First solution: the steering angle is defined in Simulink[®] and entered to TruckSim[®] through the S-function as shown in Figure 3. With this solution, the trajectories of the vehicle in the cases of the passive anti-roll bar and of the active anti-roll bar systems are often different, indicated by the effect of the wheels lift off from the road. This means that it affects the direction of the vehicle. Therefore, it is difficult to evaluate the effectiveness of the active anti-roll bar system, therefore this solution is not considered in this study.
- Second solution: there are two choices defined for the steering angle in TruckSim[®]. The 1st choice uses the closed-loop driver model, the steering angle is automatically changed to adapt to the vehicle trajectory. Here, the vehicle trajectories in the case of the passive anti-roll bar and of the active anti-roll bar systems will follow the target path which fits the driver's wishes. The 2nd choice uses the open loop driver model, the steering angles are the same for both active and passive anti-roll bar systems.

In the following validations, we use the second solution to define the steering angle.

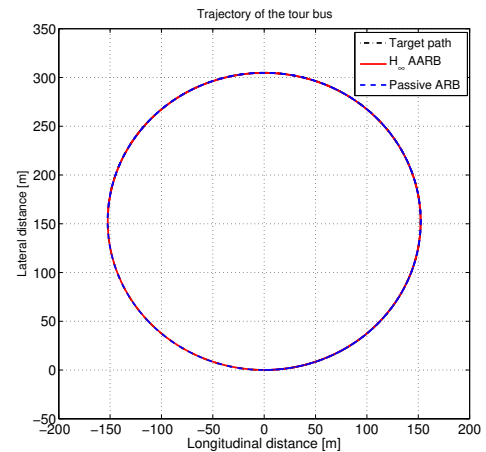


Fig. 4. Tour bus: trajectory in the circular road test.

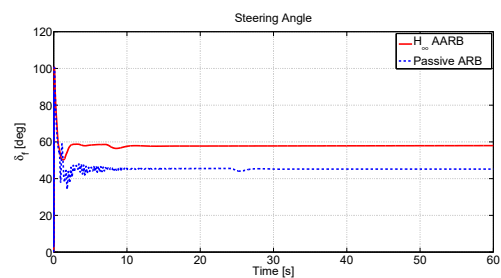


Fig. 5. Tour bus: time response of the steering angle.

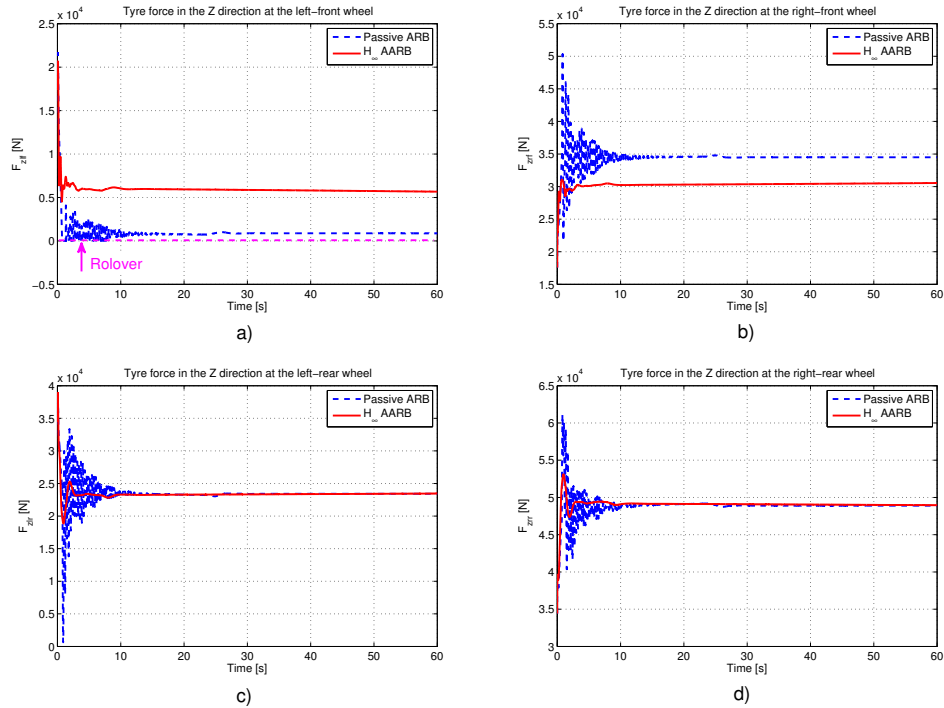


Fig. 6. Tour bus: the tyre forces in the Z direction of (a) left-front, (b) right-front, (c) left-rear, and (d) right-rear wheels.

3.2 Simulation scenario

We use the four common simulation scenarios to evaluate the effect of H_∞ active anti-roll bar system on heavy vehicles, with the objective of improving roll stability and preventing the rollover phenomenon.

- **First scenario:** Handling test on a circular test circuit with a diameter of 1000 ft and a road bank angle of 10%,
- **Second scenario:** A cornering manoeuvre with a 180 deg steering angle,
- **Third scenario:** A sine wave (\sim) steering manoeuvre,
- **Fourth scenario:** A double lane change to overtake.

Table 2 shows the validation cases of the H_∞ active anti-roll bar control system by using co-simulation between Simulink[®] and TruckSim[®]. All of the simulation scenarios with respect to a tour bus and a truck with unloaded and fully loaded options are surveyed with the different velocities. Only the two cases highlighted by the bold lettering (red color) will be shown in the following section.

Table 2. Validation cases of the H_∞ active anti-roll bar control system by using co-simulation.

Scenario	Unloaded bus	Loaded bus	Unloaded truck	Loaded truck
Circular road test	X	X	X	X
Cornering manoeuvre	X	X	X	X
Sine wave steering	X	X	X	X
Double lane change	X	X	X	X

4. VALIDATION RESULTS

In the following validations, the authors will test the H_∞ active anti-roll bar control system with two different types of heavy vehicle: a tour bus and a truck, with the fully loaded option. They use two solid suspension systems at both axles, with the

engine mounted at the rear of the tour bus, meanwhile the engine is mounted at the front of the truck. The parameters of the tour bus, as well as of the truck are found in the vehicle configuration of TruckSim[®].

4.1 Validation with a tour bus

Commercial passenger buses are probably the most popular people carrying vehicles in the world. Typically they are vehicles with two axles (bus 2A) and a capacity of 45 passengers. The legal maximum forward velocity of these buses usually reaches 130 km/h in France or more than 130 km/h in some other countries. Therefore, bus rollover is an important safety problem. Here, we consider the tour bus with the solid suspension systems for both axles and the engine mounted at the rear of the vehicle. A single tyre is used for the front axle and a dual tyre for the rear axle.

In this validation, the handling test on the circular road with a diameter of 1000 ft and a road bank angle of 10% is used to evaluate roll stability of the tour bus when it runs at 100 km/h. This is a typical form of the road surface in the proving ground, with the slope of the road (banking) toward the center of the circle. Figure 4 shows the trajectory of the tour bus in the circular road test scenario.

Figure 5 shows the time response of the steering angle. In order to ensure that the vehicle moves in the same circle with a diameter of 1000 ft, the steering angle is kept constant at 58 deg in the case of the H_∞ active anti-roll bar control system, and at 45 deg in the case of the passive anti-roll bar system. This means that the trajectories of the vehicle in the H_∞ active anti-roll bar control and the passive anti-roll bar systems coincide with the desired trajectory.

The comparison of the time response between the H_∞ active anti-roll bar control and the passive anti-roll bar systems is summarized in Table 3. We can see that, in the case of the

Table 3. Time response comparison of the tour bus.

Time responses	ϕ [deg]	ϕ_{uf} [deg]	ϕ_{ur} [deg]
H_∞ AARB	-5	0.5	1.5
Passive ARB	1.8	6.5	7.0

passive anti-roll bar, under the action of the inertial force, the tour bus rolls outwards of the corner, while it rolls into the corner in the case of the H_∞ active anti-roll bar control system. Thanks to this rolling response, the tour bus can improve its roll stability capacity. This is entirely consistent with the previous studies (Sampson and Cebon (2003a), Gaspar et al. (2004), Sampson and Cebon (2003b), Hsun-Hsuan et al. (2012), Miego and Cebon (2005b) and Yu et al. (2008)).

Figure 6 shows the time response of the tyre forces in the Z direction of all the wheels. We can see that in the case of the H_∞ active anti-roll bar control system, all the tyre forces are positive, which means that there is no wheel lift off from the road. But in the case of the passive anti-roll bar, the tyre force in the Z direction of the left-front wheel is zero from 1s to 10s (see Figure 6a). So it indicates that when the tour bus runs at 100 km/h, the left-front wheel lifts off from the road at this period of time. From these results, it shows that the H_∞ active anti-roll bar control system improves roll stability of the fully loaded tour bus, when compared to the passive anti-roll bar system.

4.2 Validation with a truck

In this validation, the cornering manoeuvre with 180 deg of steering angle is used to evaluate roll stability of the truck when it runs at 50 km/h. Even if the forward velocity at 50 km/h is not so high, this is still an emergency situation because the steering angle varies from 0 deg to 180 deg in just over 0.6s as shown in Figure 7. It is worth noting that the steering angle is kept the same in the cases of the H_∞ active anti-roll bar control and the passive anti-roll bar systems.

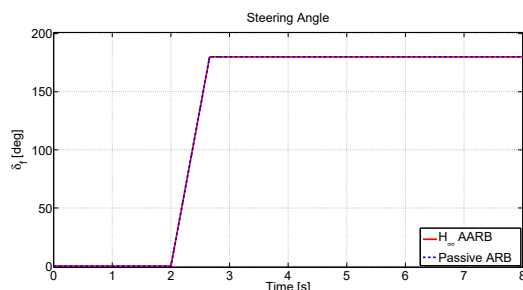


Fig. 7. Truck: time response of the steering angle.

The trajectory of the truck in the cornering manoeuvre is shown in Figure 8. In the case of the H_∞ active anti-roll bar control system, the vehicle always sticks to the target path (to point B). However, for the trajectory of the truck using the passive anti-roll bar system, it cannot follow the target path (to point A), due to the left-rear wheel lifting off the road from 3.2s to 5.5s.

Table 4. Time response comparison of the truck.

Time responses	ϕ [deg]	ϕ_{uf} [deg]	ϕ_{ur} [deg]
H_∞ AARB	7.8	6.9	7.8
Passive ARB	9.5	8.7	8.2

The comparison of the time response between the H_∞ active anti-roll bar control and the passive anti-roll bar systems is summarized in Table 4. We can see that in the case of the H_∞ active anti-roll bar control system, the roll angle of the sprung

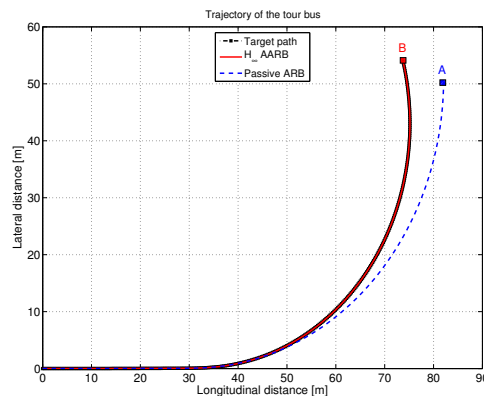


Fig. 8. Truck: trajectory in the cornering manoeuvre.

and unsprung masses are significantly reduced, when compared to the passive anti-roll bar system.

Figure 9 shows the time response of the tyre forces in the Z direction of all the wheels. We can see that in the case of the H_∞ active anti-roll bar control system, all the tyre forces are positive, which means that there is no wheel lift off from the road. But in the case of the passive anti-roll bar system, the left-rear wheel lifts off from the road from 3.2s to 5.5s (see Figure 9c). We can also see that the H_∞ active anti-roll bar control system reduces the load transfer at both axles: the tyre force in the Z direction at the left-front wheel F_{zlf} is stable around 7250 N, the right-front wheel F_{zrf} is stable around 38000 N, the left-rear wheel F_{zlr} is stable around 6500 N and the right-rear wheel F_{zrr} is stable around 70000 N. Therefore the H_∞ active anti-roll bar control system enhances the stability of the tyre forces in the Z direction for the whole time period. Moreover, there are some oscillations in the passive anti-roll bar system. These results shows that the H_∞ active anti-roll bar control system improves roll stability of the fully loaded truck.

The validation results with the nonlinear high order vehicle model for different velocities and scenarios as in Table 2 show that by using the H_∞ active anti-roll bar control system, roll stability is improved to prevent the risk of vehicle rollover, when compare with the passive anti-roll bar system.

5. CONCLUSION

In this paper, the validation of the H_∞ active anti-roll bar control system by using TruckSim[®] software is presented. The co-simulation between Matlab/Simulink[®] and TruckSim[®] allows the synthesis of the H_∞ active anti-roll bar controller in Matlab/Simulink[®] environment, and the use of the nonlinear high order vehicle model in TruckSim[®]. Specifically for this case, the outputs of TruckSim[®] (the lateral acceleration and roll rate of the sprung mass) are sent to the controller (as measurement signals) by using the H_∞ method. The outputs of the controller are the input currents of the ESVH actuators. The ESVH actuators generate the roll torques at both axles and then they are inserted into the inputs of TruckSim[®].

The simulation results in the four cases of the single unit heavy vehicle (4 × 2) (a tour bus and a truck in unloaded and fully loaded states) with the different velocities and scenarios, show that the H_∞ active anti-roll bar control system drastically improved vehicle roll stability. Thanks to good simulation results obtained by using the nonlinear vehicle model in TruckSim[®], the validation of the H_∞ active anti-roll bar control system in real-time will be of interest in the future.

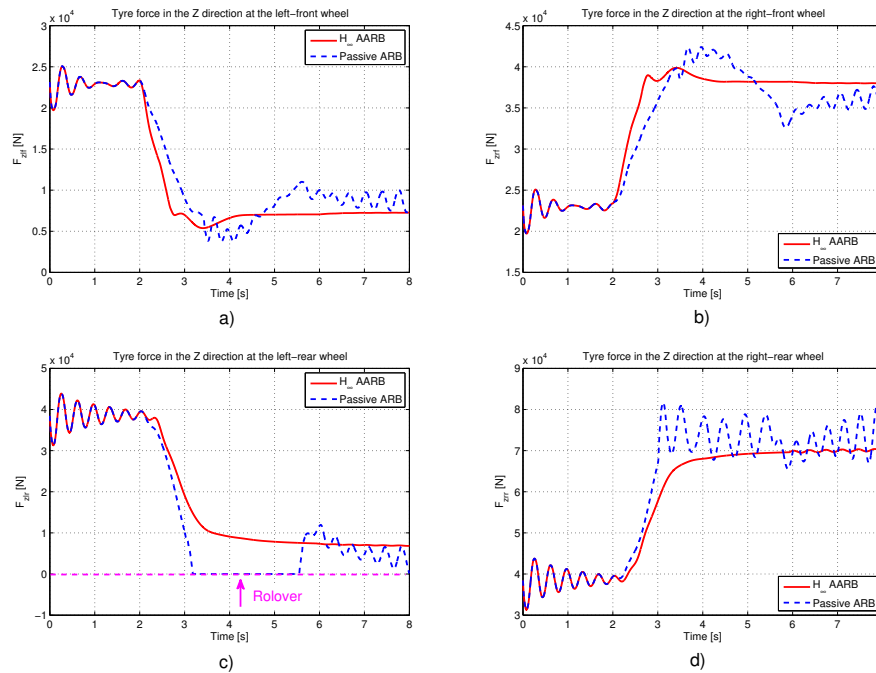


Fig. 9. Truck: the tyre forces in the Z direction of (a) left-front, (b) right-front, (c) left-rear, and (d) right-rear wheels.

Acknowledgements: This work has been supported by the GINOP-2.3.2-15-2016-00002 grant of the Ministry of National Economy of Hungary and by the European Commission through the H2020 project EPIC under grant No. 739592.

REFERENCES

- Ashfaq, A., Changjun, K., Sangho, K., Manan, K.A., Junaid, I., Zuhaib, K., Donghwan, L., and Changsoo, H. (2017). Lateral acceleration potential field function control for rollover safety of multi-wheel military vehicle with in-wheel-motors. *International Journal of Control, Automation and Systems*, 15(2), 837–847.
- Boada, M., Boada, B., Quesada, A., Gauchía, A., and Díaz, V. (2007). Active roll control using reinforcement learning for a single unit heavy vehicle. In *12th IFToMM World Congress*. Besancon, France.
- Bouteldja, M.; Sirdi, N.G.S.D.V. (2004). Stability analysis and rollover scenario prediction for tractor semi-trailer. In *International Conference on Advances in Vehicle Control and Safety AVCS04*. Italy.
- Gaspar, P., Bokor, J., and Szaszi, I. (2004). The design of a combined control structure to prevent the rollover of heavy vehicles. *European Journal of Control*, 10(2), 148–162.
- Gaspar, P., Bokor, J., and Szaszi, I. (2005). Reconfigurable control structure to prevent the rollover of heavy vehicles. *Control Engineering Practice*, 13(6), 699–711.
- Hsun-Hsuan, H., Rama, K., and Dennis, A.G. (2012). Active roll control for rollover prevention of heavy articulated vehicles with multiple-rollover-index minimisation. *Vehicle System Dynamics: International Journal of Vehicle Mechanics and Mobility*, 50(3), 471–493.
- Hussain, K., Stein, W., and J Day, A. (2005). Modelling commercial vehicle handling and rolling stability. In *Proceedings of the Institution of Mechanical Engineers, Part K: Journal of Multi-body Dynamics*. United Kingdom.
- Islam, M., He, Y., Zhu, S., and Wang, Q. (2015). A comparative study of multi-trailer articulated heavy-vehicle models. *Proceedings of the Institution of Mechanical Engineers, Part D: Journal of Automobile Engineering*, 229(9), 1200–1228.
- Miege, A. and Cebon, D. (2005a). Active roll control of an experimental articulated vehicle. *Proceedings of the Institution of Mechanical Engineers Part D Journal of Automobile Engineering*, 219(6), 791–806.
- Miege, A. and Cebon, D. (2005b). Optimal roll control of an articulated vehicle: theory and model validation. *Vehicle System Dynamics: International Journal of Vehicle Mechanics and Mobility*, 43(12), 867–884.
- Qu, G., He, Y., Sun, X., and Tian, J. (2018). Modeling of lateral stability of tractor-semitrailer on combined alignments of freeway. *Discrete Dynamics in Nature and Society*, 2018, 1–17.
- Sampson, D. and Cebon, D. (2003a). Achievable roll stability of heavy road vehicles. In *Proceedings of the Institution of Mechanical Engineers, Part D: Journal of Automobile Engineering*, volume 217, 269–287. United Kingdom.
- Sampson, D. and Cebon, D. (2003b). Active roll control of single unit heavy road vehicles. *Vehicle System Dynamics: International Journal of Vehicle Mechanics and Mobility*, 40(4), 229–270.
- Vu, V., Sename, O., Dugard, L., and Gaspar, P. (2017a). Enhancing roll stability of heavy vehicle by lqr active anti-roll bar control using electronic servo-valve hydraulic actuators. *Vehicle System Dynamics: International Journal of Vehicle Mechanics and Mobility*, 55(9), 1405–1429.
- Vu, V., Sename, O., Dugard, L., and Gaspar, P. (2017b). Multi objective H_∞ active anti-roll bar control for heavy vehicles. In *IFAC World Congress - 20th WC 2017*. Toulouse, France.
- Yu, H., Guvenc, L., and Ozguner, U. (2008). Heavy duty vehicle rollover detection and active roll control. *Vehicle System Dynamics: International Journal of Vehicle Mechanics and Mobility*, 46(6), 451–470.